

Tracking Electronic and Molecular Structural Dynamics during Dissociation of the Photocatalyst $\text{Mn}_2(\text{CO})_{10}$ via Time-Resolved X-Ray Spectroscopy

Hana Cho,^{1,2} Kiryong Hong,² Mathew L. Strader,¹ Jae Hyuk Lee,¹ Robert W. Schoenlein,¹ Nils Huse,³ and Tae Kyu Kim²

¹Ultrafast X-ray Science Lab, Chemical Sciences Division, Lawrence Berkeley National Laboratory, Berkeley, CA 94720, USA

²Department of Chemistry, Pusan National University, Geumjeong-gu, Busan 609-735, Korea

³Max Planck Research Department for Structural Dynamics, University of Hamburg & Center for Free Electron Laser Science, 22607 Hamburg, Germany

Author e-mail address: hcho@lbl.gov

Abstract: The molecular structure dynamics and transient valence charge distribution during the photo-dissociation of the photocatalyst $\text{Mn}_2(\text{CO})_{10}$ are revealed via time-resolved x-ray spectroscopy at the Mn K-edge, combined with quantum chemistry simulations.

OCIS codes: (000.1570) General; (300.6530) Ultrafast Spectroscopy; (300.6560) X-ray Spectroscopy

We have conducted the first time-resolved x-ray absorption spectroscopy studies of the transient electronic and molecular structure of bimetallic $\text{Mn}_2(\text{CO})_{10}$ following photodissociation. $\text{Mn}_2(\text{CO})_{10}$ is one of the simplest binuclear metal carbonyl complexes and is a prototype for understanding solution photolysis of organometallic compounds with metal-metal bonds. Moreover, $\text{Mn}_2(\text{CO})_{10}$ is an important photocatalyst in numerous synthetic reactions, facilitating bond cleavage through formation of stable $\cdot\text{Mn}(\text{CO})_5$ photoradicals with high quantum yield [1,2]. Previous studies have applied ultrafast visible and infrared spectroscopy to characterize both the structure and reactivity of the species in order to determine the reaction mechanisms [3].

However, the vibrational complexity of large molecular frameworks and the typical broad featureless electronic spectra limit the information on electronic and molecular structure that can be extracted. We apply transient XANES spectroscopy to provide information on changes in valence charge distribution/spin state, and transient EXAFS to reveal the local molecular structure [4,5]. Comparison of x-ray spectra with quantum chemistry calculations reveals a detailed picture of the transient local electronic and molecular structure in time and energy.

Our studies focus on the homolytic photo-dissociation of $\text{Mn}_2(\text{CO})_{10}$, in organic solvents. Upon photoexcitation two dissociation pathways are possible, leading to the generation of two different products via metal-metal or metal-ligand bond breaking: (i) $\text{Mn}_2(\text{CO})_{10} \rightarrow 2\cdot\text{Mn}(\text{CO})_5$ and (ii) $\text{Mn}_2(\text{CO})_{10} \rightarrow \text{Mn}_2(\text{CO})_9 + \text{CO}$ [7,8]. The relative quantum yield for these two channels depends on the excitation wavelength. While both $\text{Mn}_2(\text{CO})_9$ and the $\cdot\text{Mn}(\text{CO})_5$ radical are produced upon excitation with ultraviolet wavelengths, long wavelength excitation at 400 nm yields predominantly the monometallic product $\cdot\text{Mn}(\text{CO})_5$ (dissociation time: <120 fs) which subsequently equilibrates with the solvent within 10 ps and persists for many nanoseconds before recombination [8-10]. Thus, 400 nm excitation enables the investigation of the dynamics of the transient $\cdot\text{Mn}(\text{CO})_5$ product free from interference of other products.

We have conducted the time-resolved x-ray measurements in a 15 mM flowing solution of $\text{Mn}_2(\text{CO})_{10}$ in 2-propanol at the manganese K-edge using beamline 6.0.1 at the Advanced Light Source (ALS). Differential XANES and EXAFS spectra monitor changes in molecular structure and a valence charge density distribution during radical formation. The *ab-initio* program FEFF 9.05 was used for

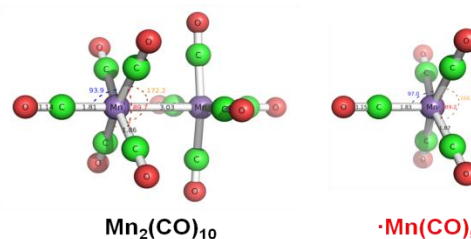


Fig. 1. Molecular structures of $\text{Mn}_2(\text{CO})_{10}$ and the $\cdot\text{Mn}(\text{CO})_5$ radical.

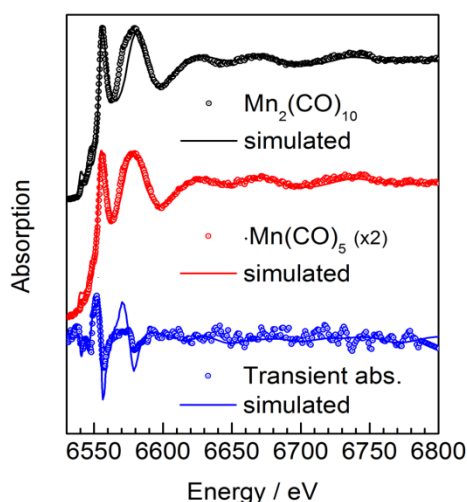


Fig. 2. XANES and EXAFS spectra at the Mn K-edge. The reconstructed spectrum of photo-generated $\cdot\text{Mn}(\text{CO})_5$ radical was generated from the Mn K-edge differential spectrum at 400 ps delay after photodissociation with $f=12\%$ [6]. The open circles are experimental data and the solid lines are fits from the real space multiple scattering code FEFF 9.05 using DFT optimized structures.

XANES and EXAFS simulations at the Mn K-edge. The structures of $\text{Mn}_2(\text{CO})_{10}$ and the $\cdot\text{Mn}(\text{CO})_5$ radical (as input to the FEFF simulations) were calculated using density functional theory (DFT). The experimental and computed Mn K-edge spectrum of $\text{Mn}_2(\text{CO})_{10}$ in the electronic ground-state and the spectrum of the transient photoproduct $\cdot\text{Mn}(\text{CO})_5$ are shown in Fig. 2. The measured differential absorption spectrum (blue) has been used to compute the transient Mn K-edge spectrum of $\cdot\text{Mn}(\text{CO})_5$. The *ab initio* FEFF simulations show very good agreement with experiment, and the spectral changes at the Mn K-edge are thus directly related to the modifications of the molecular structure [11]. From these comparisons we find that the $\text{Mn}_2(\text{CO})_{10}$ molecule is distorted from the octahedral coordinated (D_{4d}) configuration, and the 5-fold coordinated $\cdot\text{Mn}(\text{CO})_5$ radical is square pyramid (C_{4v}) [12] rather than trigonal bipyrimid (D_{3h}) structure (See Fig. 1). Thus, the structure of the photodissociated $\cdot\text{Mn}(\text{CO})_5$ radical closely resembles one half of the $\text{Mn}_2(\text{CO})_{10}$ following the metal-metal bond breaking, with very little structural change of the carbonyl ligand cage around the Mn center.

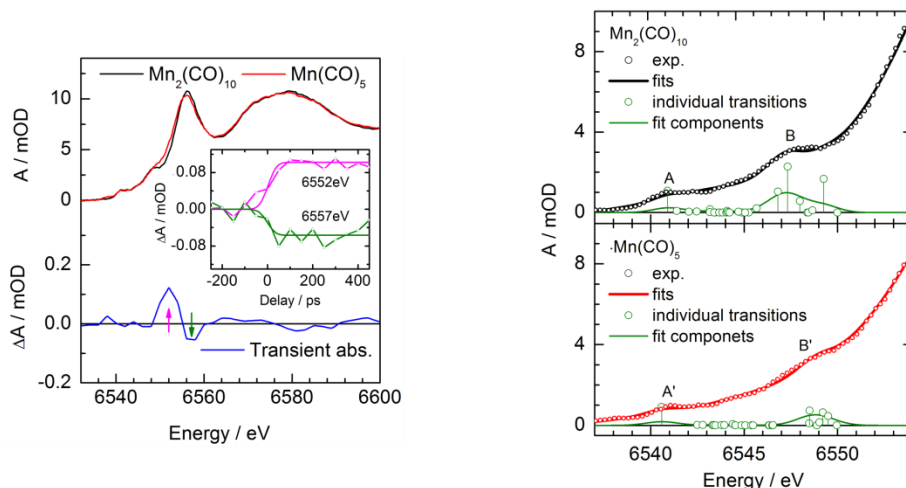


Fig. 3. Left: Kinetics of the difference XANES for $\text{Mn}_2(\text{CO})_{10}$ and $\cdot\text{Mn}(\text{CO})_5$ radical. Inset: time-response at 6552 eV and 6557 eV. Right: Comparison between experimental (open circles), fit components (green lines) and calculated fits (solid lines) of pre-edge spectra at the Mn K-edge for $\text{Mn}_2(\text{CO})_{10}$ (black) and the $\cdot\text{Mn}(\text{CO})_5$ radical by TD-DFT (ORCA simulation).

As illustrated in Fig. 3, the x-ray spectrum shows an intense dipole-allowed transition ($1s \rightarrow 4p$) at 6556 eV, with distinct changes in the intensity and the position of this peak following photoexcitation (blue). Since the oxidation state of the metal does not change after the bond breaking, the major cause of the energy shift is attributed to changes in either the bond strength of the first-sphere ligands, or in orbital occupancy due to mixing of the metal d orbitals with ligand valence orbitals [13]. The amplitude of main-peak decreases due to change of orbital occupancy and the peak shifts to lower energy which corresponds to reduced energy splitting (antibonding MO is shifted to lower energy) in the $\cdot\text{Mn}(\text{CO})_5$ radical. The changes of pre- and main-edges at the Mn K-edge region associated with electronic contributions in metal $3d$, $4p$ orbitals and ligand $2p$ orbitals are attributed to minor structural modifications. The inset time-scans reflect the formation of the $\cdot\text{Mn}(\text{CO})_5$ radical within the 70 ps resolution as determined by the x-ray probe pulse duration.

Transient x-ray absorption in combination with computational chemistry codes are powerful new tools for understanding valence electronic structural changes, and can provide new insight into the nature of the bonding associated with the formation of photofragments. This approach may be applied to directly follow electronic and molecular structural changes in a variety of chemical and biological systems.

- [1] R. Bianchi, G. Gervasio, D. Marabello, *Inorg. Chem.* **39**, 2360-2366 (2000).
- [2] R. D. Adams, M. Huang, W. Huang, *Organometallics* **16**, 4479-4485 (1997).
- [3] T. J. Meyer, J. V. Caspar, *Chem. Rev.* **85**, 187-218 (1985).
- [4] S. C. Kohn, J. M. Charnock, C. M. B. Henderson, G. N. Greaves, *Contrib. Mineral. Petrol.* **105**, 359-368 (1990).
- [5] M. Croft, D. Sills, M. Greenblatt, C. Lee, S. -W. Cheong, K. V. Ramanujachary, D. Tran, *Phys. Rev. B* **55**, 8726-8732 (1997).
- [6] M. Sarakha, G. Ferraudi, *Inorg. Chem.* **38**, 4605-4607 (1999).
- [7] T. Kobayashi, H. Ohtani, H. Noda, S. Teratani, H. Yamazaki, K. Yasufuku, *Organometallics* **5**, 110-113 (1986).
- [8] J. Z. Zhang, C. B. Harris, *J. Chem. Phys.* **95**, 4024-4032 (1991).
- [9] D. A. Steinhurst, A. P. Baronavski, J. C. Osrutsky, *Chem. Phys. Lett.* **361**, 513-519 (2002).
- [10] C. R. Baiz, P. L. McRobbie, N. K. Preketes, K. J. Kubarych, E. Geva, *J. Phys. Chem. A* **113**, 9617-9623 (2009).
- [11] B. Gilbert, B. H. Frazer, A. Belz, P. G. Conrad, K. H. Nealon, D. Haskel, et al., *J. Phys. Chem. A* **107**, 2839-2847 (2003).
- [12] A. Rosa, G. Ricciardi, E. J. Baerends, D. J. Stufkens, *Inorg. Chem.* **34**, 3425-3432 (1995).
- [13] H. Visser, E. Anxolabéhère-Mallart, U. Bergmann, P. Glatzel, J. H. Robblee, S. P. Cramer, et al., *J. Am. Chem. Soc.* **123**, 7031-7039 (2001).